Supplemental Data

DOTA Conjugate with an Albumin-Binding Entity Enables the First Folic Acid–Targeted ^{177}Lu-Radionuclide Tumor Therapy in Mice

Cristina Müller[1*], Harriet Struthers[2], Christian Winiger[2], Konstantin Zhernosekov[1], Roger Schibli[1,2]

[1] *Center for Radiopharmaceutical Sciences ETH-PSI-USZ, Paul Scherrer Institute, Villigen-PSI, Switzerland*

[2] *Department of Chemistry and Applied Biosciences, ETH Zurich, Zurich, Switzerland*

[3]*Laboratory of Radiochemistry and Environmental Chemistry, Paul Scherrer Institute, Villigen-PSI, Switzerland*

* Corresponding author:

Dr. Cristina Müller
Center for Radiopharmaceutical Sciences ETH-PSI-USZ
Paul Scherrer Insitute
5232 Villigen-PSI
Switzerland

e-mail: cristina.mueller@psi.ch
phone: +41-56-310 44 54
fax: +41-56-310 28 49

1. Organic Synthesis of Folate Compound cm09

Folate-based radiotracers are excreted primarily via kidneys. Due to the expression of the FR in the proximal tubules (*1*, *2*), a high accumulation of radioactivity is usually found in the renal tissue after injection of folate radioconjugates (*3*). We hypothesized that extension of the circulation time of folate radioconjugates would increase their tumor uptake and reduce accumulation of radioactivity in the kidneys. Thus, a novel folic acid conjugate was synthesized by installation of a small-molecular weight albumin binding entity (*4*). It was supposed that reversible interaction of the folate radioconjugate with serum albumin would increase the circulation time of the radioconjugate, which would otherwise be quickly excreted via the kidneys.

1.1. Experimental Procedure

The albumin binding functionality was synthesized by reaction of *p*-iodo-4-phenylbutric acid (**S1**) with α-Boc-protected lysine followed by Boc-deprotection to yield compound **S2** (Supplemental Fig. 1).

Compound **S2** was then conjugated with propargyl glycine to introduce an azide functionality. Deprotection of the product resulted in compound **S3** which was further reacted with α-methyl-Boc-protected glutamic acid. Deprotection of the amino group gave compound **S4**. N2-*N*,*N*-dimethylaminomethylene-10-formyl-pteroic acid (**S5**) was activated with HBTU. After 1 h of stirring at 0°C, the slurry was added dropwise to a solution of compound **S4** and NEt_3 in DMF. After 3-4 h the solvent was evaporated under reduced pressure and the compound was purified by column chromatography using mixtures of CH_2Cl_2 and MeOH as the eluent. The protected folate conjugate (**S6**) was fully deprotected in MeOH/NaOH(aq) at pH 12.5 to give compound **S7** (Supplemental Fig. 1). The reactions were monitored by HPLC and MS.

4-Azidobutane-1-amine was reacted with compound **S7** using catalytic amounts of copper acetate and sodium ascorbate to give compound **S8** (Supplemental Fig. 2). The free amine group in compound **S8** was reacted with N-hydroxysuccinimide (NHS)-activated DOTA in DMF in the presence of DIPEA for several hours at 40 °C to give the final folate compound **cm09**. The reaction was monitored by HPLC and MS. The product was purified by precipitation from a basic aqueous solution on addition of HCl to decrease the pH.

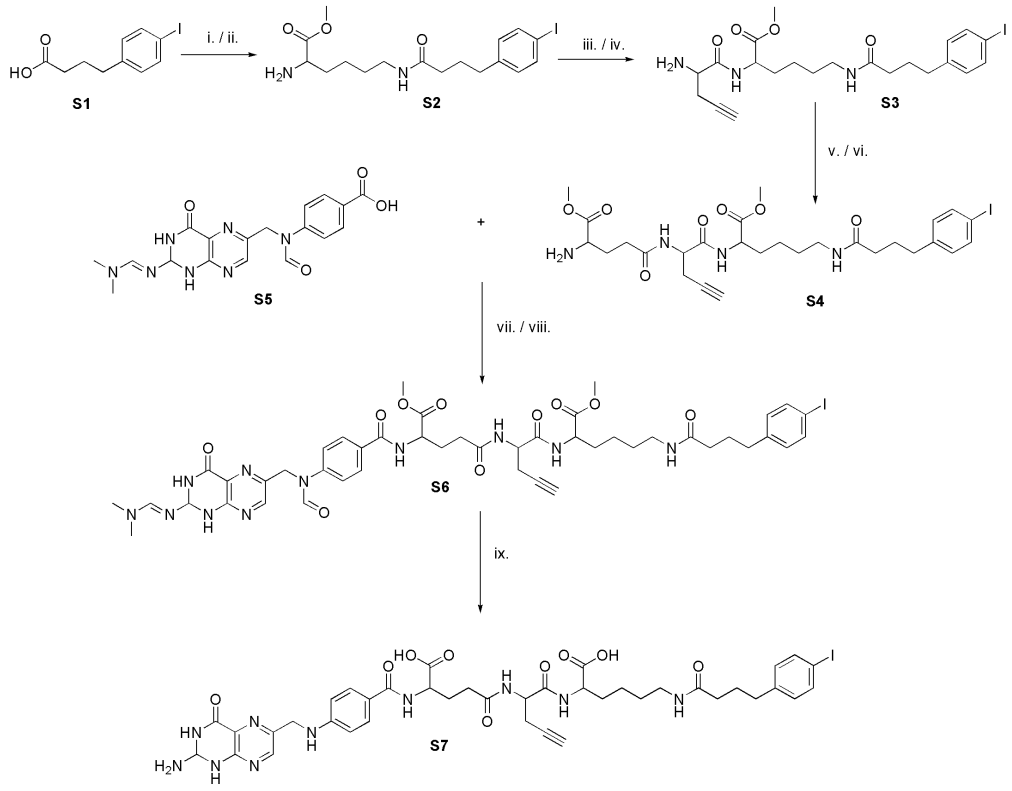

SUPPLEMENTAL FIGURE 1. i) Boc-Lys-OMe, HBTU, DMF, NEt_3, 75% yield ii) TFA, CH_2Cl_2 iii) Boc-Pra-OH, HBTU, DMF, NEt_3 iv) TFA, CH_2Cl_2 v) Boc-Glu-OMe, HBTU, DMF, NEt_3 vi) TFA, CH_2Cl_2 vii) HBTU, DMF, NEt_3 viii) DMF, NEt_3, 44% yield ix) MeOH/NaOH(aq.) pH 12.5.

1.2. Results and Conclusion of Organic Synthesis of Folate Conjugate cm09

Synthesis of compound **cm09** was carried out in 11 steps (Supplemental Fig. 1 and 2) resulting in an overall yield of ~ 10%. The compound was obtained in > 95% purity as confirmed by HPLC. LC/MS electrospray ionization (ESI): *m/z* 1437.44 $[C_{60}H_{83}IN_{18}O_{16}]H^+$ (calculated 1437.51).

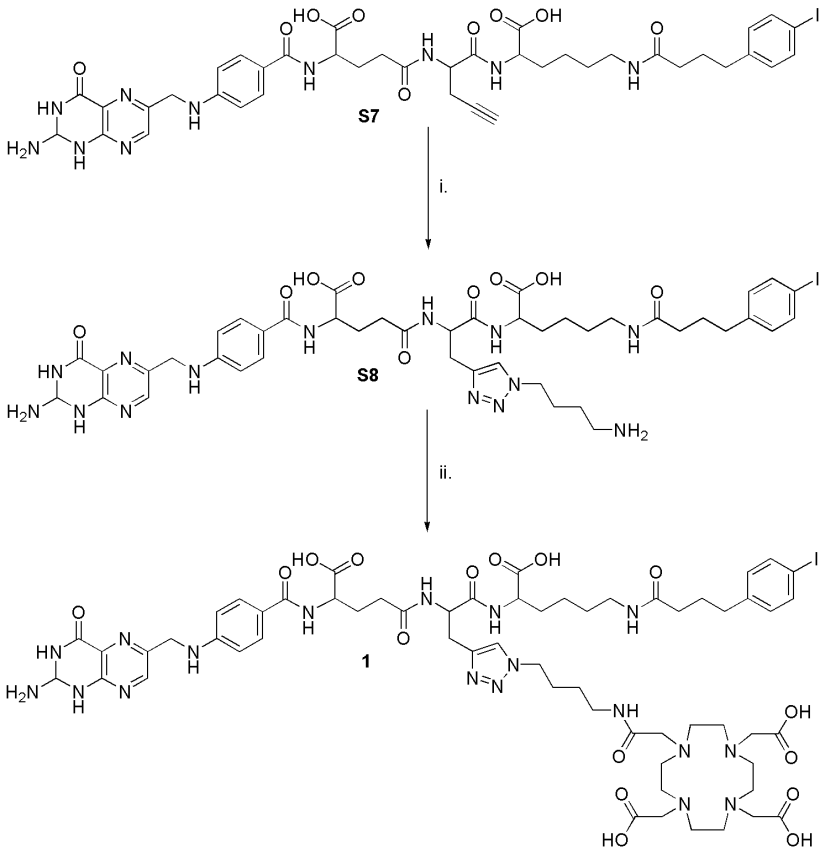

SUPPLEMENTAL FIGURE 2. i) 4-azido-butyl-1-amine, $Cu(OAc)_2 \cdot H_2O$, Na ascorbate, $tBuOH/H_2O$, 43% yield ii) N-hydroxy-succinimide-DOTA, DMF, DIPEA, 46% yield.

2. Organic Synthesis of Folate Compound EC0800

The control compound DOTA-Bz-folate, hereafter referred to as **EC0800** (Supplemental Fig. 3) was kindly provided by Dr. Christopher P. Leamon, Endocyte Inc. The preparation and evaluation of **EC0800** has been reported previously (*3*).

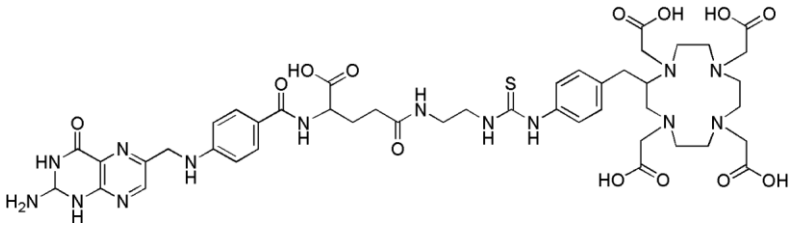

SUPPLEMENTAL FIGURE 3. Chemical structure of **EC0800** employed as a control folate conjugate.

3. In Vitro Radiolysis

The stability of folate vitamins is known to be influenced by several factors such as temperature, pH, oxygen, (ultraviolet) light, metal ions, antioxidants, heating and ionizing radiation (*5*-*7*). Radiolysis of radiopharmaceuticals is a common phenomenon (*8*) which has also been observed with folate-based radioconjugates (unpublished observation). For a therapeutic application relatively high doses of radioactivity are formulated in small volumes of buffer or saline suitable for injection. It is crucial to be able to ensure the integrity of the radioconjugate until injection into the animal. The purpose of this experiment was therefore to investigate potential radiolysis of ^{177}Lu-**cm09** under conditions that correspond to an injection solution suitable for therapeutic purposes.

3.1. Experimental Procedure

Folate compounds **EC0800** and **cm09** were radiolabeled with ^{177}Lu at a specific activity of 40 MBq/nmol. The radiotracers were prepared as they would be if they were used for the injection of mice at a dose of 20 MBq in 100 μL PBS. Solutions of 80 MBq ^{177}Lu-**cm09** or ^{177}Lu-**EC0800** in a volume of 400 μL PBS were kept at room temperature. At different time points (t = 0, 1 h, 2 h, 4 h, 24 h and 48 h) after preparation, an aliquot was taken and analyzed by HPLC.

3.2. Results and Conclusion of In Vitro Radiolysis Experiments

HPLC analysis showed that there was no decomposition of ^{177}Lu-**cm09** over the first 4 h. At later time points a small peak (R_t = 17.6 min) of a radioactive compound of unknown composition (~ 3.5% at 24 h and ~ 5.6% at 48 h) was detected. In the case of the control compound (^{177}Lu-**EC0800**) already the first analysis after preparation showed a radioactive side product (R_t = 10.7 min) which accounted for ~ 15% and which was presumably a result of immediate radiolysis. The relative amount of this pre-peak remained almost stable over the first 4 h after preparation of ^{177}Lu-**EC0800**. However, at later time points the percentage of radiolytic product increased to ~ 53%. These results clearly indicate the superior stability of ^{177}Lu-**cm09** over ^{177}Lu-**EC0800**. The albumin binding entity appears to stabilize the radioconjugate against radiolytic decomposition.

4. Octanol/PBS pH 7.4 Distribution Coefficient (log D)

Based on existing data obtained with radiolabeled folate conjugates, it can be concluded that hydrophilic compounds (e.g. ^{111}In/^{177}Lu-DOTA-click-folate (*9*), ^{67}Ga-DOTA-Bz-folate (*3*)) are more favorable because of their almost exclusive elimination via the kidneys, while lipophilic conjugates tend to accumulate in the intestinal tract (e.g. ^{99m}Tc(CO)$_3$-folates (*10*-*12*)). Unspecific

accumulation in the abdomen would be unfavorable with respect to a therapeutic application because with a high dose burden to abdominal organs and tissues risk of toxicity is high.

4.1. Experimental Procedure

The distribution coefficient (logD) of both ^{177}Lu-radiolabeled DOTA-folates (^{177}Lu-**cm09** and ^{177}Lu-**EC0800**) was determined using a previously published procedure (*9*). In brief, a sample (~ 500 kBq) of either the HPLC-purified ^{177}Lu-**cm09** or ^{177}Lu-**EC0800** was mixed with an equal volume of PBS (pH 7.4) and octanol (1500 µL). The vials were vortexed vigorously for 1 min and then centrifuged for 6 min to achieve phase separation. The concentration of radioactivity in a defined volume of each layer was measured in a γ-counter. The distribution coefficient was expressed as the logarithm of the ratio of counts per minute (cpm) measured in the octanol phase to the cpm measured in the PBS phase. The values reported are the mean of four independent measurements (± SD), each performed in quadruplicate.

4.2. Results and Conclusion of the Determination of the Distribution Coefficient (logD)

The logD value obtained for ^{177}Lu-**cm09** (- 4.25 ± 0.41) was slightly higher than for ^{177}Lu-**EC0800** (- 4.81 ± 0.36). These numbers indicated the hydrophilic character of both radiofolates which was comparable to the previously evaluated ^{111}In-radiolabeled DOTA-click-folate (log D = - 4.21 ± 0.11 (*9*)). Although the albumin binding entity of ^{177}Lu-**cm09** is a relatively lipophilic molecule, the hydrophilic DOTA-chelator dominated the overall characteristics of this folate radioconjugate. The expected consequences of such low logD values were predominant excretion of these folate radioconjugates via the kidneys.

5. In Vitro Cell Experiment to Investigate FR-Binding Affinity

It is known from the literature that folic acid in its oxidized version binds with a higher affinity to the FR than the reduced physiological form (5-methyltetrahydrofolate, 5-MTHF) (*13-15*). To release folic acid from FRs an acidic washing buffer with a pH value below 3.5 is required. However, since the pH value in the endosome is higher, folic acid is not released in the cell interior which is in clear contrast to the behavior of physiological 5-MTHF. To prove equally high FR-binding affinity of ^{177}Lu-**cm09** and ^{177}Lu-**EC0800** compared to folic acid we investigated on whether the FR-bound internalized fraction was recycled back with the receptor to the cell surface over time.

5.1. Experimental Procedure

KB cells were seeded in 12-well plates to grow overnight (~ 700,000 cells in 2 ml FFRPMI medium/well). After removal of the supernatant, HPLC-purified ^{177}Lu-**cm09** or ^{177}Lu-**EC0800** (~ 38 kBq, 8 pmol) was added in 1 mL FFRPMI (without supplements) to each well and the well-plates were incubated for 2 h at 37°C. After removal of the supernatant, cells were washed once with acidic stripping buffer (*16*) followed by PBS. The amount of radioactivity measured in acid-stripped cells of one well-plate corresponding to the internalized fraction of ^{177}Lu-**cm09** and ^{177}Lu-**EC0800**, respectively, was set to 100%. In the remaining well-plates FFRPMI medium (without supplements) was added and cells were incubated for 2 h at 37°C again. Then, cells were washed with stripping buffer and PBS. Cells of one well-plate were lysed and measured in a gamma-counter whereas cells of another well-plate were incubated again and the described procedure was repeated once more before lysis and measuring those cells as well in a gamma-counter.

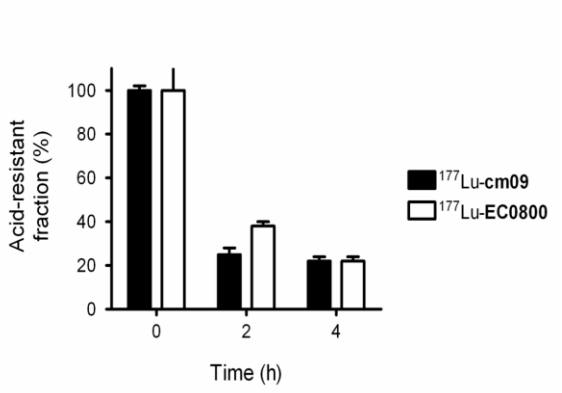

SUPPLEMENTAL FIGURE 4. The internalized (acid-resistant) fraction of ^{177}Lu-**cm09** and ^{177}Lu-**EC0800** after 2 h incubation with KB cells was set to 100%. Two h and 4 h later the cells were washed again with an acidic stripping buffer to release folate radioconjugates which were recycled back to the surface for determination of the acid-resistant fraction.

5.2. Results and Conclusion of In Vitro Cell Experiment to Investigate FR-Binding Affinity

With this experiment it was shown that after internalization both folate radioconjugates remained bound to the FR and recycled back to the cellular surface. After release of the acid-labile fraction using an acidic buffer a new equilibrium between the acid-resistant and acid-labile fraction was reached during incubation at 37°C. Repetition of this procedure resulted in release of the acid-labile fraction again resulting in a reduction of the acid-resistant pool over time (Supplemental Fig. 4). These findings indicate a strong binding affinity of ^{177}Lu-**cm09** or ^{177}Lu-**EC0800** to the

FR which is in the same range as the affinity of folic acid which is not released into the cytoplasm of the cell interior.

6. Biodistribution Studies of ^{177}Lu-EC0800

In its ^{67}Ga-radiolabeled form, folate conjugate **EC0800** has been previously investigated by our group (*3*). However, for comparison of the in vivo data obtained with ^{177}Lu-**cm09** it was necessary to use the control compound (**EC0800**) in its ^{177}Lu-radiolabeled form (^{177}Lu-**EC0800**) in case the overall tissue distribution of the radiofolate was influenced by the different coordination chemistry of gallium and lutetium.

6.1. Experimental Procedure

KB tumor bearing nude mice were intravenously injected with ^{177}Lu-**EC0800** (3 MBq, 1 nmol, 100 μL). At different time points (1 h, 4 h, 24 h, 48 h and 72 h) after injection, mice were euthanized. Organs and tissues of interest were collected and counted in a γ-counter to determine the uptake of ^{177}Lu-**EC0800** expressed as [% ID/g]-values.

SUPPLEMENTAL TABLE 1

Biodistribution of ^{177}Lu-**EC0800** (3 MBq, 1 nmol) in KB Tumor Bearing Nude Mice

	^{177}Lu-EC0800				
	1 h p.i.	4 h p.i.	24 h p.i.	48 h p.i.	72 h p.i.
blood	0.26 ± 0.05	0.11 ± 0.02	0.04 ± 0.04	0.02 ± 0.01	0.03 ± 0.00
lung	1.22 ± 0.05	0.81 ± 0.05	0.62 ± 0.07	0.41 ± 0.05	0.44 ± 0.03
spleen	0.76 ± 0.19	0.89 ± 0.78	0.24 ± 0.06	0.43 ± 0.02	0.67 ± 0.50
kidneys	**72.95 ± 11.18**	**73.68 ± 3.50**	**57.95 ± 3.75**	**51.22 ± 6.92**	**43.31 ± 2.58**
stomach	2.25 ± 0.25	1.75 ± 0.14	1.06 ± 0.07	0.92 ± 0.13	0.75 ± 0.16
intestines	0.69 ± 0.08	0.43 ± 0.09	0.30 ± 0.08	0.22 ± 0.04	0.24 ± 0.06
liver	5.13 ± 2.28	2.53 ± 0.57	1.68 ± 0.50	1.90 ± 0.33	2.11 ± 0.15
salivary glands	7.56 ± 0.18	4.88 ± 1.17	2.58 ± 0.57	2.37 ± 0.20	2.15 ± 0.10
muscle	1.21 ± 0.35	1.21 ± 0.15	0.70 ± 0.08	0.44 ± 0.02	0.47 ± 0.10
bone	1.23 ± 0.24	1.17 ± 0.12	0.72 ± 0.16	0.44 ± 0.04	0.50 ± 0.06
tumor	**7.05 ± 1.04**	**7.52 ± 1.15**	**7.00 ± 1.22**	**5.05 ± 0.71**	**3.02 ± 0.38**
tumor-to-blood	27.56 ± 3.42	72.47 ± 21.96	161.2 ± 58.6	265.4 ± 52.9	116.34 ± 15.48
tumor-to-liver	1.57 ± 0.63	3.11 ± 0.92	4.14 ± 1.42	2.74 ± 0.65	1.43 ± 0.10
tumor-to-kidney	0.10 ± 0.02	0.10 ± 0.01	0.12 ± 0.03	0.09 ± 0.01	0.07 ± 0.01

6.2. Results and Conclusion of Biodistribution Studies of ^{177}Lu-EC0800

The results of the biodistribution studies performed with ^{177}Lu-**EC0800** are shown in Supplemental Table 1. The data are comparable to those previously obtained with the same folate conjugate (**EC0800**) radiolabeled with [^{67}Ga]gallium (*3*). Maximum uptake in KB tumor xenografts (7.52 ± 0.71% ID/g) was found 4 h p.i. of ^{177}Lu-**EC0800** and the majority was retained over 48 h (5.05 ± 1.15% ID/g). Accumulation in the kidneys was very high (> 70% ID/g) shortly after injection of ^{177}Lu-**EC0800**, while wash-out of radioactivity from the kidneys was very slow, resulting in unfavorably low tumor-to-kidney ratios (< 0.15) at all time points. However, clearance from blood and background organs (lung, spleen, stomach, intestines, muscle and bone) was relatively fast. Beside the kidneys, significant accumulation of radioactivity was only found in the salivary glands (4.88 ± 1.17 % ID/g, 4 h p.i.) which are known to express the FR (*12*) and in the liver (2.53 ± 0.57% ID/g, 4 h p.i.), an organ that does not express the FR but accumulates folate vitamins for storage purposes in a physiological process.

7. Tumor-to-Background Ratios of ^{177}Lu-cm09 in Comparison to ^{177}Lu-EC0800

In order to visualize tumor-to-background ratios of ^{177}Lu-**cm09** in comparison to the tumor-to-background ratios of ^{177}Lu-**EC0800** the values have been combined and presented in graphs of the tumor-to-blood, tumor-to-liver and tumor-to-kidney ratios (Supplemental Fig. 5). In addition, tumor-to-kidney ratios were determined by quantification of the SPECT data acquired at 1h, 4h, 24h and 72h p.i.

7.1. Experimental Procedure

The experimental procedures of the biodistribution studies performed with KB tumor-bearing mice after injection of ^{177}Lu-**cm09** and ^{177}Lu-**EC0800** are described in "Biodistribution Studies" of the main manuscript and the Supplemental Data, section 6.

Quantification of the SPECT data was performed with InVivoScope postprocessing software (version 1.44, Bioscan, Inc.). Accumulation of radioactivity [MBq] in a defined tissue volume [cm^3] was determined for tumors and kidneys and expressed as the tumor-to-kidney ratios (= activity concentration in tumors [MBq/cm^3] divided by activity concentrations in the kidneys [MBq/cm^3]).

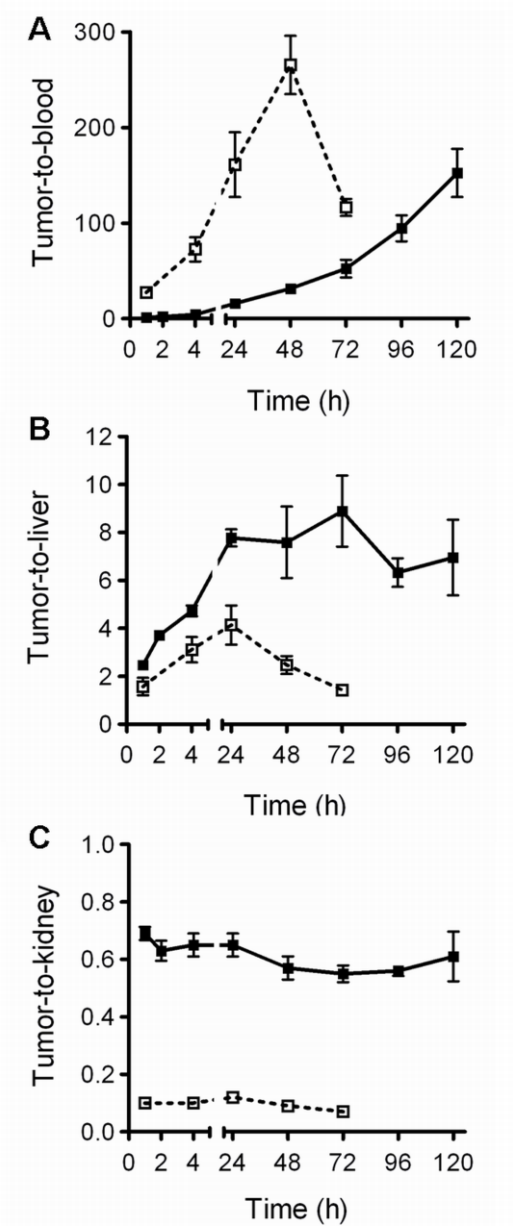

SUPPLEMENTAL FIGURE 5. The graphs show tumor-to-background ratios of ^{177}Lu-**cm09** (■) and ^{177}Lu-**EC0800** (□) over time. A: tumor-to-blood ratios, B: tumor-to-liver ratios and C: tumor-to-kidney ratios.

7.2. Results and Conclusion

Due to the albumin binding properties of ^{177}Lu-**cm09** the tumor-to-blood ratios were slowly and constantly increasing over time reaching the highest value at the latest time points of investigation. In contrast, tumor-to-blood ratios of ^{177}Lu-**EC0800** were increasing quickly reaching a maximum value 48 h after injection. On the other hand, tumor-to-liver and tumor-to-

kidney ratios were clearly higher after injection of ^{177}Lu-**cm09** compared with the values observed after injection of ^{177}Lu-**EC0800**. These findings demonstrate the favorable characteristics of ^{177}Lu-**cm09**, particularly with regard to the tumor-to-kidney ratios which is the most critical issue of the FR-targeting strategy using folic acid radioconjugates for therapeutic purposes. The tumor-to-kidney ratios of ^{177}Lu-**cm09** determined by SPECT quantification were clearly higher (0.96; 0.90; 1.06; 1.19) compared to the ratios obtained for ^{177}Lu-**EC0800** (0.12; 0.20; 0.22; 0.27) at 1 h, 4 h, 24 h and 72 h p.i.

8. Variation of the Molar Amount of Injected Folate Conjugate ^{177}Lu-cm09

It is generally recognized that the molar amount of injected substance of peptide-based, vitamin-based and other small-molecular-weight targeting agents can significantly affect the uptake of radioactivity in malignant and healthy tissues (*17-20*). The receptors in receptor-positive normal tissue are saturated with a smaller amount of targeting agent than is necessary to saturate receptors on the tumor. Furthermore the targeting agent in its unlabeled version may promote tumor growth; therefore, it is of interest to inject radiopharmaceuticals at high specific activities i.e. a small molar amount of targeting agent. With these experiments, we wanted to investigate the effect of variable molar amounts of folate conjugate **cm09** on the tumor and kidney uptake of radioactivity.

8.1. Experimental Procedure

The folate conjugate **cm09** was radiolabeled to obtain a specific activity of 1 MBq per 0.25 nmol. Preparation of the various injection solutions was carried out by addition of unlabeled folate conjugate **cm09** to the solution of ^{177}Lu-**cm09**. Tissue distribution studies were performed 4 h after intravenous injection of ^{177}Lu-**cm09**.

8.2. Results and Conclusion

Biodistribution data were similar for the different amounts of injected folate conjugate **cm09** (Supplemental Table 2). Interestingly, there was a tendency towards higher tumor uptake with a higher amount of injected compound **cm09**. This trend was in contrast to the data that are usually seen with other targeting agents (*17, 19*) and might be ascribed to the albumin binding properties of **cm09**. The lowest amount of injected folate conjugate (0.25 nmol) clearly resulted in a lower overall uptake in FR-positive organs and tissues whereas the injection of molar amounts in the range of 0.5 nmol to 1.0 nmol resulted in almost identical [%ID/g]-values. Based on these data we decided to employ a molar amount of 0.5 nmol folate conjugate **cm09** per mouse for therapy

studies. This amount appeared most suitable as it was high enough to inject the large doses of radioactivity required for therapeutic purposes.

SUPPLEMENTAL TABLE 2

Biodistribution 4 h p.i. of ^{177}Lu-**cm09** in KB Tumor Bearing Nude Using Different Amounts of Folate Conjugate

	^{177}Lu-**cm09**			
	0.25 nmol	0.50 nmol	0.75 nmol	1.00 nmol
blood	4.01 ± 0.47	4.38 ± 0.95	5.31 ± 1.00	5.82 ± 1.69
lung	2.56 ± 0.29	2.70 ± 0.24	3.10 ± 0.60	3.61 ± 1.06
spleen	1.24 ± 0.02	1.18 ± 0.19	1.36 ± 0.12	1.45 ± 0.34
kidneys	**23.67 ± 2.24**	**28.05 ± 1.35**	**27.13 ± 1.69**	**31.50 ± 6.64**
stomach	1.56 ± 0.31	1.45 ± 0.25	1.50 ± 0.18	1.61 ± 0.25
intestines	0.71 ± 0.16	0.90 ± 0.20	0.74 ± 0.19	0.74 ± 0.18
liver	4.53 ± 0.26	3.86 ± 0.65	3.92 ± 0.95	4.63 ± 0.03
salivary glands	5.40 ± 0.65	6.23 ± 0.69	5.98 ± 0.79	6.04 ± 0.92
muscle	1.34 ± 0.19	1.26 ± 0.06	1.20 ± 0.11	1.31 ± 0.33
bone	1.36 ± 0.18	1.23 ± 0.14	1.43 ± 0.33	0.37 ± 0.32
tumor	**13.95 ± 1.34**	**18.12 ± 1.80**	**17.68 ± 2.11**	**20.02 ± 3.22**
tumor-to-blood	3.54 ± 0.64	4.32 ± 1.15	3.37 ± 0.36	3.63 ± 0.97
tumor-to-liver	3.11 ± 0.47	4.73 ± 0.39	4.74 ± 1.37	4.31 ± 0.48
tumor-to-kidney	0.59 ± 0.09	0.65 ± 0.07	0.65 ± 0.06	0.64 ± 0.07

9. ^{177}Lu-cm09 Injection Mixture with Human Serum Albumin or Mouse Serum

Despite the presence of an albumin-binding entity, a significant fraction of ^{177}Lu-**cm09** was still found in the renal tissue even at early time points after application. This was the result of the free (unbound) fraction of ^{177}Lu-**cm09** which was filtered through kidneys. We hypothesized that mixing the radioconjugate with serum albumin before administration would potentially reduce the fraction of ^{177}Lu-**cm09** filtered and thus further reduce renal accumulation of radioactivity. Two approaches were investigated. In the first experiment, the radiofolate was mixed with solutions of human serum albumin before injection. In the second experiment, the radiofolate was mixed with mouse serum before administration.

9.1. Experimental Procedure

The various injection solutions were prepared by addition of ^{177}Lu-**cm09** to a solution of 2% or 10% serum albumin in NaCl 0.9%. For further experiments ^{177}Lu-**cm09** was dissolved in PBS mixed with mouse serum (65 volume%). Mice were dissected 4 h after intravenous injection of ^{177}Lu-**cm09** (~ 2 MBq, 1.0 nmol, 100 μL per mouse).

SUPPLEMENTAL TABLE 3

Biodistribution 4 h p.i. of ^{177}Lu-DOTA-**cm09** Mixed with Human Serum Albumin in KB Tumor Bearing Nude Mice

	^{177}Lu-cm09			
	2 % HSA 4 h p.i.	2 % HSA 24 h p.i.	10 % HSA 4 h p.i.	10 % HSA 24 h p.i.
blood	5.39 ± 0.96	1.39 ± 0.44	4.15 ± 0.37	1.40 ± 0.22
lung	3.33 ± 0.22	1.46 ± 0.41	2.57 ± 0.39	1.80 ± 0.73
spleen	1.36 ± 0.12	0.87 ± 0.18	1.23 ± 0.19	0.83 ± 0.12
kidneys	**29.66 ± 6.06**	**29.50 ± 1.66**	**29.70 ± 5.62**	**31.64 ± 2.45**
stomach	1.46 ± 0.11	1.10 ± 0.23	1.76 ± 0.21	1.13 ± 0.09
intestines	0.83 ± 0.09	0.53 ± 0.11	0.69 ± 0.06	0.47 ± 0.14
liver	3.85 ± 0.64	2.59 ± 0.37	3.78 ± 0.58	3.04 ± 0.49
salivary glands	6.69 ± 0.30	4.18 ± 0.57	5.89 ± 2.02	4.37 ± 0.25
muscle	1.30 ± 0.10	0.89 ± 0.16	1.35 ± 0.20	1.22 ± 0.17
bone	1.49 ± 0.22	0.98 ± 0.19	1.30 ± 0.22	1.01 ± 0.02
tumor	**19.79 ± 2.42**	**18.76 ± 2.16**	**16.85 ± 1.54**	**18.59 ± 3.23**
tumor-to-blood	3.71 ± 0.39	14.06 ± 2.30	3.46 ± 1.73	11.03 ± 5.48
tumor-to-liver	5.24 ± 1.05	7.27 ± 0.31	3.74 ± 1.85	4.99 ± 2.71
tumor-to-kidney	0.68 ± 0.08	0.63 ± 0.04	0.50 ± 0.25	0.49 ± 0.24

9.2. Results and Conclusion

Mixing ^{177}Lu-**cm09** with a solution of different concentrations of human serum albumin (2% or 10%) did not have a positive effect on the overall tissue distribution (Supplemental Table 3). Compared to the injection of ^{177}Lu-**cm09** in PBS only, which resulted in a kidney accumulation of ~ 28% ID/g, 4 h p.i. and ~ 30% ID/g, 24 h p.i., the values obtained in this study were very similar (Supplemental Table 3). The uptake in tumor tissue was also unchanged. Injection of ^{177}Lu-**cm09** in mouse serum did not have a major impact on the tissue distribution either (data not shown). Kidney uptake was in the same range (32.62 ± 5.85% ID/g, 4 h p.i.) as found after the injection of ^{177}Lu-**cm09** in PBS only (28.05 ± 1.35% ID/g, 4 h p.i.). Based on these data it was

concluded that renal uptake of radioactivity is not reduced by mixing ^{177}Lu-**cm09** with serum albumin or mouse serum before administration.

10. Intraperitoneal and Subcutaneous Injection of ^{177}Lu-cm09

Repeated administration of radiolabeled compounds or their combination with chemotherapeutics or kidney protecting agents might be of interest in a therapeutic setting. This would require several intravenous injections to the same test animal. Intravenous injection is technically challenging and undesirable because of potential physical damage to the tail vein and an increased risk of infection. Therefore, it might be of interest to employ alternative administration routes. Recently, we observed that the application route (intravenous vs. intraperitoneal vs. subcutaneous) did not have a significant impact on the tissue distribution of ^{67}Ga-radiolabeled **EC0800** (*3*). These findings were in agreement with those determined with peptide-based radioconjugates (*17*). However, it remained unclear as to whether these conclusions would be transferable to folate conjugate **cm09,** which unlike **EC0800** has albumin binding properties. Therefore, we investigated the tissue distribution of radioactivity after intraperitoneal and subcutaneous application of ^{177}Lu-**cm09** and evaluated whether this approach is advantageous when compared with intravenous administration of ^{177}Lu-**cm09**.

10.1. Experimental Procedure

Biodistribution studies were performed with mice that received ^{177}Lu-**cm09** (~ 2 MBq, 1.0 nmol, 100 μL per mouse) via the subcutaneous or intraperitoneal administration route. The animals were sacrificed 4 h after injection of ^{177}Lu-**cm09**. Selected tissues and organs were collected, weighed, and counted for radioactivity in a γ-counter.

10.2. Results and Conclusion

The results of these experiments are shown in Supplemental Table 4. Variation of the administration route had only minor effects on the overall tissue distribution of ^{177}Lu-**cm09**. There was a trend of reduced uptake of radioactivity in tumors and kidneys after subcutaneous injection of ^{177}Lu-**cm09** compared to the results obtained after intravenous injection of ^{177}Lu-**cm09**. In contrast, retention of radioactivity in the blood was higher after subcutaneous and intraperitoneal injection of ^{177}Lu-**cm09** compared to the value obtained after intravenous injection. The tumor-to-background ratios were similar for all three routes of administration. Overall, intravenous administration appeared to be the most favorable application route with regard to high tumor uptake and maximum tumor-to-background ratios.

SUPPLEMENTAL TABLE 4

Comparison of Tissue Distribution Data for ^{177}Lu-**cm09**, 4 h After Intravenous (i.v.), Intraperitoenal (i.p.) and Subcutaneous (s.c.) Injection in KB Tumor Bearing Nude Mice

	^{177}Lu-cm09		
	i.v.	s.c.	i.p.
blood	4.38 ± 0.95	5.96 ± 0.43	6.26 ± 0.99
lung	2.70 ± 0.24	3.40 ± 0.21	3.54 ± 0.14
spleen	1.18 ± 0.19	1.33 ± 0.18	1.51 ± 0.05
kidneys	**28.05 ± 1.35**	**23.05 ± 4.02**	**25.58 ± 1.25**
stomach	1.45 ± 0.25	1.68 ± 0.49	2.09 ± 0.29
intestines	0.90 ± 0.20	1.03 ± 0.43	1.02 ± 0.26
liver	3.86 ± 0.65	3.17 ± 0.17	3.51 ± 0.22
salivary glands	6.23 ± 0.69	6.07 ± 0.23	7.85 ± 1.16
muscle	1.26 ± 0.06	1.28 ± 0.12	1.51 ± 0.31
bone	1.23 ± 0.14	1.15 ± 0.10	1.37 ± 0.20
tumor	**18.12 ± 1.80**	**12.97 ± 2.71**	**17.30 ± 0.66**
tumor-to-blood	4.32 ± 1.15	2.18 ± 0.45	2.81 ± 0.42
tumor-to-liver	4.73 ± 0.39	4.08 ± 0.76	4.95 ± 0.32
tumor-to-kidney	0.65 ± 0.07	0.57 ± 0.12	0.68 ± 0.04

11. Biodistribution Studies of ^{177}Lu-cm09 in Combination with Pemetrexed

In our previous work we demonstrated that a preinjection of the antifolate pemetrexed reduced kidney uptake of radiofolates significantly without affecting tumor accumulation of radioactivity. By such a pharmacological intervention the tumor-to-kidney ratios were significantly improved (*9, 21-23*). The purpose of these experiments was to investigate whether the tumor-to-kidney ratios of ^{177}Lu-**cm09** would be further improved by pre-administered pemetrexed.

11.1. Experimental Procedure

Pemetrexed (Alimta®, LY231514, Eli Lilly) was diluted with NaCl 0.9% according to the instructions of the manufacturer. Biodistribution studies were performed with KB tumor bearing nude mice which received pemetrexed (400 μg in 100 μL saline) 1 h prior to ^{177}Lu-**cm09** (~ 1 MBq, 1.0 nmol per mouse). Mice were sacrificed at 4 h, 24 h, 48 h and 72 h after injection of ^{177}Lu-**cm09**. Selected tissues and organs were collected, weighed, and counted for radioactivity in a γ-counter. Statistical analyses were performed by using a t-test (Microsoft Excel software). All

analyses were two-tailed and considered as type 3 (two sample unequal variance). A p-value of < 0.05 was considered statistically significant.

11.2. Results and Conclusion

The tissue distribution data found in these experiments are shown in Supplemental Table 5. Preinjection of pemetrexed reduced kidney uptake 4 h after injection of ^{177}Lu-**cm09** to about 60% of control values ($p < 0.005$). In contrast, no significant ($p > 0.1$) reduction of renal accumulation of ^{177}Lu-**cm09** was found at later time points after injection (24 h, 48 h and 72 h p.i.). These findings could be attributed to the fact that ^{177}Lu-**cm09** circulates much longer in the blood stream than pemetrexed and hence the blocking effect on renal accumulation of ^{177}Lu-**cm09** was only possible during the first hours after injection. Most probably, repeated injection of pemetrexed would allow reducing kidney uptake also at later time points after injection of ^{177}Lu-**cm09**. However, from a logistic point of view such an approach would be difficult and in addition, increasing the frequency of pemetrexed injection risks toxicity from pemetrexed.

SUPPLEMENTAL TABLE 5

Biodistribution of ^{177}Lu-**cm09** in KB Tumor Bearing Nude Mice

	^{177}Lu-cm09			
	PMX* 4 h p.i.	PMX* 24 h p.i.	PMX* 48 h p.i.	PMX* 72 h p.i.
blood	6.49 ± 1.50	1.21 ± 0.31	0.41 ± 0.15	0.31 ± 0.0
lung	4.43 ± 0.56	1.19 ± 0.18	0.74 ± 0.14	0.57 ± 0.02
spleen	1.54 ± 0.52	0.74 ± 0.03	0.64 ± 0.07	0.50 ± 0.09
kidneys	**16.81 ± 2.25**	**25.52 ± 6.88**	**22.81 ± 2.48**	**21.34 ± 0.03**
stomach	1.60 ± 0.26	0.72 ± 0.07	0.46 ± 0.13	0.39 ± 0.01
intestines	1.15 ± 0.58	0.29 ± 0.09	0.15 ± 0.04	0.14 ± 0.01
liver	2.64 ± 0.33	2.56 ± 0.60	2.49 ± 0.47	1.26 ± 0.48
salivary glands	6.26 ± 1.14	2.98 ± 0.56	2.39 ± 0.18	1.85 ± 0.48
muscle	1.16 ± 0.02	1.01 ± 0.01	0.55 ± 0.07	0.47 ± 0.05
bone	1.29 ± 0.20	0.82 ± 0.31	0.47 ± 0.04	0.40 ± 0.04
tumor	**18.43 ± 6.68**	**17.29 ± 3.31**	**17.21 ± 2.76**	**9.87 ± 1.46**
tumor-to-blood	2.86 ± 0.81	14.74 ± 4.12	45.48 ± 16.16	32.95 ± 9.33
tumor-to-liver	6.95 ± 2.19	6.81 ± 0.90	7.16 ± 1.99	8.21 ± 1.86
tumor-to-kidney	1.07 ± 0.25	0.69 ± 0.06	0.76 ± 0.15	0.46 ± 0.07

* PMX injected 1 h prior to the radiofolate

12. Estimation of Absorbed Dose in Tumors and Kidneys

In order to get an idea about the radioactive dose burden of ^{177}Lu-**cm09** to KB tumor xenografts and kidneys, we made a dose estimation for this tumor mouse model. Only the self-radiation dose was taken into account for these tissues.

12.1. Experimental Procedure

To estimate the equivalent absorbed radiation dose for ^{177}Lu-**cm09** in tumor xenografts and kidneys, the following assumptions were made: (i) the cumulative radioactivity was calculated from integrated AUCs (MBq·s) of biodistribution data expressed in non decay-corrected percent injected dose [%ID] per organ mass (100 mg for tumor, 150 mg for each kidney), (ii) the adsorbed radiation dose in tumor xenografts was assessed for a sphere of 100 mg using the Unit Density Sphere Model from RADAR (www.doseinfo-radar.com) and (iii) the absorbed radiation dose in kidneys was assessed using S-values from Larson et al. (*24*).

The absorbed dose (mGy/MBq) was calculated by multiplying the AUC (s; normalized to 1 MBq ID) with the S-value (mGy/MBq·s). The dose (mGy) was calculated by multiplying the absorbed dose (mGy/MBq) by the amount of radioactivity injected.

12.2. Results and Conclusion of the Dose Calculation

In the case of ^{177}Lu-**cm09**, an absorbed dose of 1.80 Gy/MBq was estimated for KB tumor xenografts. It results in an absorbed dose of ~ 36 Gy in tumors for a single injection of 20 MBq. Systematic investigations of the tumor response in relation to the injected amount of radioactivity are addressed in the next part of our study.

For kidneys, an absorbed dose of of 3.44 Gy/MBq was estimated, resulting in a dose of about 69 Gy for injection of 20 MBq ^{177}Lu-**cm09**. A renal dose of ~ 25 Gy is generally accepted as the safe upper limit for external beam radiation (*25*). In the case of targeted radionuclide therapy with ^{177}Lu and ^{90}Y higher absorbed kidney doses are also considered safe (*26-28*). In patients, however, the radiation-induced loss of renal function is only expected to become clinically evident years after application of targeted radionuclide therapy (*27*). Clearly it will be necessary to investigate the potential damage to the kidneys caused by application of ^{177}Lu-**cm09** in mice over a time period of several months, in a similar manner to that in which it was investigated for ^{177}Lu-DOTA-octreotate in rats by Rolleman et al. (*29*).

13. Pilot Therapy Study with ^{177}Lu-cm09

The aim of this pilot study was to investigate the therapeutic effect of ^{177}Lu-**cm09** on the tumor growth of nude mice bearing human KB tumor xenografts. For this purpose we chose a single injection of a dose of 20 MBq per mouse.

13.1. Experimental Procedure

Eight mice were inoculated with 4.5 Mio KB tumor cells on each shoulder at day -5. At day 0 when the average tumor size reached a volume of 113 ± 43 mm^3, four mice received an intravenous injection of PBS only (A: control group) whereas the remaining four mice received 20 MBq/0.5 nmol ^{177}Lu-**cm09** (B: treated group). Over a time period of 45 days, body weight and tumor size ([0.5 x (L x W^2)]) were measured every other day.

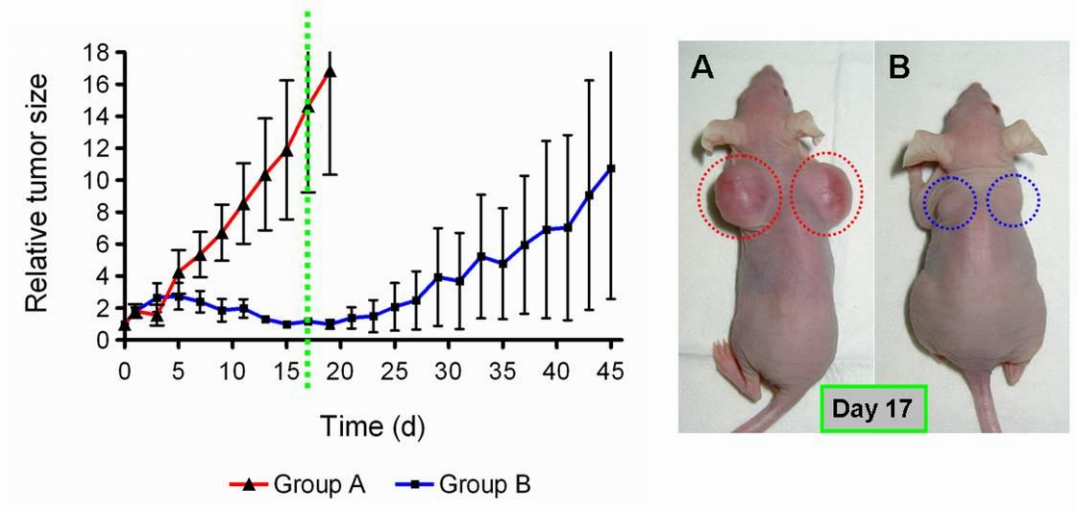

SUPPLEMENTAL FIGURE 6. The graph shows the relative size of tumor xenografts from control mice (group A, n = 4) and mice that received 20 MBq of ^{177}Lu-**cm09** (group B, n = 4) on day 0. Tumor growth was monitored over a time period of 45 days. Pictures were taken from a representative mouse of each group at day 17 after therapy.

13.2. Results and Conclusion of the Pilot Therapy Study with ^{177}Lu-cm09

The relative tumor growth of each group of animals is shown in Supplemental Fig. 6. In group A, where mice had received only PBS (control group), KB tumor xenografts grew continuously and in all cases reached the endpoint criterion of a volume of 1500 mm^3 and required euthanasia. Two of the mice were euthanized at day 19 and the other two at day 21 when tumor xenografts reached a volume of > 1500 mm^3. Among mice that received 20 MBq of ^{177}Lu-**cm09** (group B) tumor growth was significantly inhibited compared to the tumor growth of control mice. On day 21 when all of the control mice had been euthanized due to oversized tumors, the average relative

tumor size of group B was only 1.2. Moreover, in three of the four treated mice one tumor disappeared completely but in two cases one of those tumors started to grow again around day 33. At day 37 one of the treated mice had to be euthanized due to an oversized tumor. At day 45 when the study was terminated three of four mice of group B were still alive with an average relative tumor size below 5.9. Taken together, a significant inhibition of tumor growth and a prolonged survival were observed in mice that received ^{177}Lu-**cm09** compared to those that received PBS only. These findings clearly indicated an antitumor efficacy of ^{177}Lu-**cm09**. Compared to the main therapy study which is reported in the main article we observed a slightly faster tumor growth in both, mice of the control group and mice which received radionuclide therapy. These findings might be the result of a somewhat larger tumor volume in mice at the beginning of the pilot therapy study compared to the average tumor volume of mice from the main study.

14. Photos of Mice of the Main Therapy Study

A further therapy study which included 5 groups (A-E) of 5 mice each is reported in the main article. Eighteen days after the start of therapy, pictures were taken in order to visualize the difference in tumor size in mice from each group (Supplemental Fig. 7).

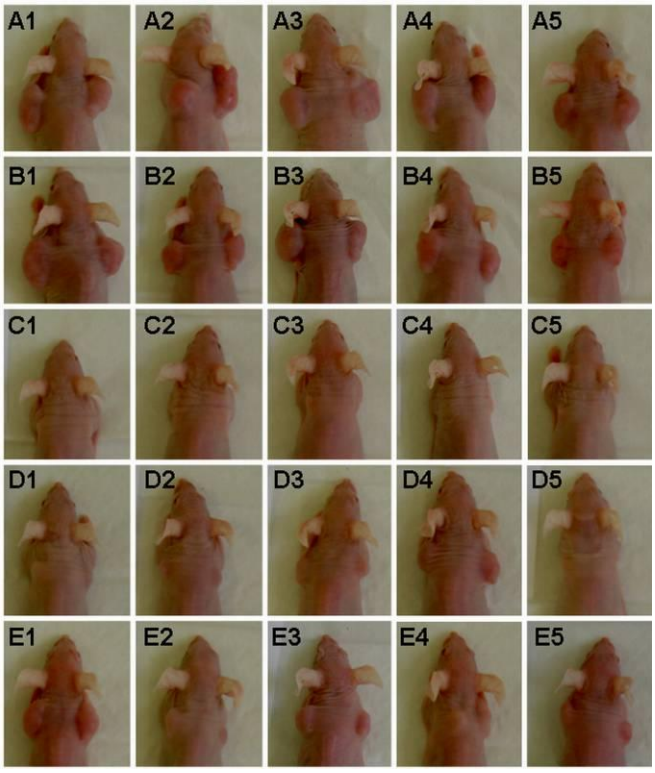

SUPPLEMENTAL FIGURE 7. Photos of mice (1-5) of each group (A-E) at day 18 after therapy start.

15. In Vitro Autoradiography and Eosin/Hematoxylin Staining

In vitro autoradiography studies were performed with tumor sections of mice from each group of the main therapy study in order to investigate potential loss of FR-density after therapy.

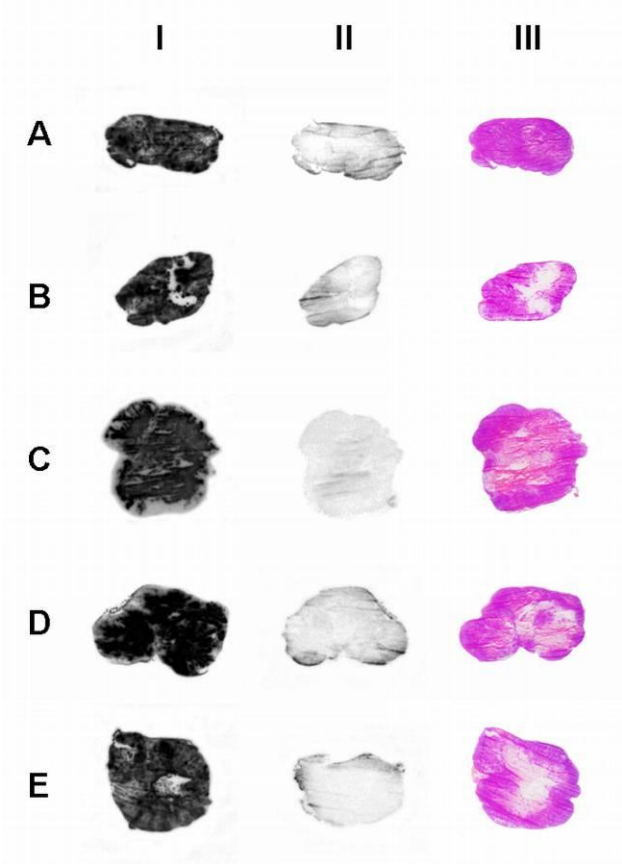

SUPPLEMENTAL FIGURE 8. In vitro autoradiography of frozen sections from tumors collected from one mouse from each group (A-E) using ^{177}Lu-DOTA-folate alone (I) or ^{177}Lu-DOTA-folate combined with excess folic acid (II) and eosin/hematoxylin staining (III) of adjacent tumor sections.

15.1. Experimental Procedure

In vitro autoradiography studies were performed on frozen sections of tumors from mice of group A-D. The slides with tissue sections were preincubated in Tris-HCl buffer (170 mM, pH 7.6, with 5 mM $MgCl_2$) with 0.25 % (w/v) bovine serum albumin (BSA) for 10 min at room temperature. The sections were subsequently incubated with 100 µL of ^{177}Lu-folate (0.5 MBq/mL) in Tris HCl buffer containing 1 % BSA for 60 min at room temperature. After incubation, the sections were rinsed twice for 5 min in cold Tris-HCl buffer (with 25 % BSA), then washed for 5 min in pure Tris-HCl buffer, and finally rinsed with cold distilled water. The sections were air-dried and exposed to phosphor imaging screens (type SR, Packard Instruments Co.) for 1 h in x-ray

cassettes. The screens were then read by a phosphor imager (Cyclone; Packard, Instruments Co.) to reveal distribution of radioactivity throughout the sections. Eosin/hematoxylin staining was performed with adjacent tumor sections and the staining pattern was compared to the corresponding autoradiogram.

15.2. Results and Conclusion of In Vitro Autoradiography and Eosin/Hematoxylin Staining

Autoradiography studies showed binding of the ^{177}Lu-labeled folate radioconjugate throughout the tissue sections of tumors from all groups. Incubation of the sections with excess folic acid reduced radioactive binding to background levels (Supplemental Fig. 8). Eosin/hematoxylin staining of adjacent sections was performed to discriminate intact sections from damaged tissue and intact cells with nuclei from necrotic tissue.

16. Plasma Chemistry

In order to account for potential abnormal or toxic reactions of the mice upon ^{177}Lu-therapy, creatinine (CRE), blood urea nitrogen (BUN) and alkaline phosphatase (ALP) were measured in plasma prepared from blood samples taken from the sublingual vein of the mice.

16.1. Experimental Procedure

At day 20 after the first injection and before euthanasia (group A-E), blood was drawn from the sublingual vein of at least 3 mice from each group (A-E). Plasma samples were prepared by centrifugation of the blood samples which were collected in heparinized vials (Microvette, 200 mL Sarstedt, Nümbrecht, Germany) and stored at -35°C until analysis. Plasma levels of CRE, BUN and ALP were determined in 10 μL plasma samples using a Fuji Dri-Chem 40000i analyzer (Polymed Medical Center AG, Switzerland).

16.2. Results and Conclusion of Plasma Chemistry

Plasma values determined for mice of each group are listed in Supplemental Table 6. Plasma creatinine was < 18 μmol/L in all of the mice, even at a late stage of the experiment. Values of blood urea nitrogen were in the range of untreated non-tumor-bearing nude mice (5.18 ± 0.85 mmol/L at day 10; 7.09 ± 0.83 mmol/L at day 60, unpublished data). Levels of alkaline phophatase increased with tumor burden and hence were lowest in mice in group C. Values of untreated non-tumor-bearing nude mice were as low as 111 ± 31 U/L at day 10 and 65 ± 19 U/L at day 60 (unpublished data).

SUPPLEMENTAL TABLE 6

Plasma Parameters: creatinine (CRE), blood urea nitrogen (BUN) and alkaline phosphatase (ALP)

CRE	A	B	C	D	E
µmol/L	PBS	cm09	^{177}Lu-**cm09**	^{177}Lu-**cm09**	^{177}Lu-**cm09**
	-	-	1 x 20 MBq	2 x 10 MBq	3 x 7 MBq
day 20	< 18	< 18	< 18	< 18	< 18
terminal	< 18	< 18	< 18	< 18	< 18
BUN	A	B	C	D	E
mmol/L	PBS	cm09	^{177}Lu-**cm09**	^{177}Lu-**cm09**	^{177}Lu-**cm09**
	-	-	1 x 20 MBq	2 x 10 MBq	3 x 7 MBq
day 20	4.20 ± 0.03	6.06 ± 1.49	6.07 ± 0.40	5.22 ± 0.47	4.01 ± 0.70
terminal	6.68 ± 0.68	5.18 ± 0.76	8.31 ± 1.57	7.28 ± 1.02	6.44 ± 1.69
ALP	A	B	C	D	E
U/L	PBS	cm09	^{177}Lu-**cm09**	^{177}Lu-**cm09**	^{177}Lu-**cm09**
	-	-	1 x 20 MBq	2 x 10 MBq	3 x 7 MBq
day 20	208 ± 42	247 ± 65	97 ± 18	105 ± 16	76 ± 10
terminal	321 ± 81*	287 ± 66	178 ± 179	383 ± 76	270 ± 117

17. FR-Binding of Folate Radioconjugates in the Choroid Plexus of the Brain

SPECT/CT images showed accumulation of radioactivity in FR-positive KB tumor xenografts and in the kidneys where the FR is expressed in the proximal tubule cells (*1, 30*). Accumulation of folate radioconjugates in the brain was not visible on these SPECT images although it is well known that the choroid plexus expresses the FR at high levels (*30, 31*). For visualization of the choroid plexus via SPECT other imaging parameters would be required. In previous studies performed in our group it was possible to visualize accumulation of a ^{99m}Tc-radiofolate in the choroid plexus of a mouse which clearly indicates FR-specific binding of folate-based radiopharmaceuticals (*12*).

Given the important role of FRs for maintenance of sufficient folate levels in the cerebrospinal fluid (*32*) the risk of damage to these receptors by particle-emitting folate radioconjugates should be kept in mind and will require thorough investigations in case of a clinical application of ^{177}Lu-**cm09** or other folic acid targeted radiopharmaceuticals.

References

1. Holm J, Hansen SI, Hoiermadsen M, Bostad L. A high-affinity folate binding-protein in proximal tubule cells of human kidney. *Kidney Int.* 1992;41:50-55.
2. Birn H, Spiegelstein O, Christensen EI, Finnell RH. Renal tubular reabsorption of folate mediated by folate binding protein 1. *J Am Soc Nephrol.* 2005;16:608-615.
3. Müller C, Vlahov IR, Santhapuram HK, Leamon CP, Schibli R. Tumor targeting using ^{67}Ga-DOTA-Bz-folate - investigations of methods to improve the tissue distribution of radiofolates. *Nucl Med Biol.* 2011;38:715-723.
4. Dumelin CE, Trussel S, Buller F, et al. A portable albumin binder from a DNA-encoded chemical library. *Angew Chem Int Ed Engl.* 2008;47:3196-3201.
5. Off MK, Steindal AE, Porojnicu AC, et al. Ultraviolet photodegradation of folic acid. *J Photochem Photobiol B.* 2005;80:47-55.
6. Vorobey P, Steindal AE, Off MK, Vorobey A, Moan J. Influence of human serum albumin on photodegradation of folic acid in solution. *Photochem Photobiol.* 2006;82:817-822.
7. Araujo MM, Marchioni E, Bergaentzle M, et al. Irradiation stability of folic acid in powder and aqueous solution. *J Agric Food Chem.* 2011;59:1244-1248.
8. Chen J, Linder KE, Cagnolini A, et al. Synthesis, stabilization and formulation of [^{177}Lu]Lu-AMBA, a systemic radiotherapeutic agent for gastrin releasing peptide receptor positive tumors. *Appl Radiat Isot.* 2008;66:497-505.
9. Müller C, Mindt TL, de Jong M, Schibli R. Evaluation of a novel radiofolate in tumour-bearing mice: promising prospects for folate-based radionuclide therapy. *Eur J Nucl Med Mol Imaging.* 2009;36:938-946.
10. Müller C, Hohn A, Schubiger PA, Schibli R. Preclinical evaluation of novel organometallic ^{99m}Tc-folate and ^{99m}Tc-pteroate radiotracers for folate receptor-positive tumour targeting. *Eur J Nucl Med Mol Imaging.* 2006;33:1007-1016.
11. Müller C, Schubiger PA, Schibli R. Synthesis and in vitro/in vivo evaluation of novel ^{99m}Tc(CO)$_3$-folates. *Bioconjug Chem.* 2006;17:797-806.
12. Müller C, Forrer F, Schibli R, Krenning EP, de Jong M. SPECT study of folate receptor-positive malignant and normal tissues in mice using a novel ^{99m}Tc-radiofolate. *J Nucl Med.* 2008;49:310-317.

13. Parker N, Turk MJ, Westrick E, Lewis JD, Low PS, Leamon CP. Folate receptor expression in carcinomas and normal tissues determined by a quantitative radioligand binding assay. *Anal Biochem.* 2005;338:284-293.
14. Kamen BA, Smith AK. A review of folate receptor alpha cycling and 5-methyltetrahydrofolate accumulation with an emphasis on cell models in vitro. *Adv Drug Deliv Rev.* 2004;56:1085-1097.
15. Kamen BA, Wang MT, Streckfuss AJ, Peryea X, Anderson RGW. Delivery of folates to the cytoplasm of MA104 cells is mediated by a surface membrane receptor that recycles. *J Biol Chem.* 1988;263:13602-13609.
16. Ladino CA, Chari RVJ, Bourret LA, Kedersha NL, Goldmacher VS. Folate-maytansinoids: target-selective drugs of low molecular weight. *Int J Cancer.* 1997;73:859-864.
17. Bernhardt P, Kolby L, Johanson V, Nilsson O, Ahlman H, Forssell-Aronsson E. Biodistribution of ^{111}in-DTPA-D-Phe^{1}-octreotide in tumor-bearing nude mice: influence of amount injected and route of administration. *Nucl Med Biol.* 2003;30:253-260.
18. Schmitt A, Bernhardt P, Nilsson O, Ahlman H, Kolby L, Forssell-Aronsson E. Differences in pharmacokinetics between therapeutic and trace amounts of ^{177}Lu-DOTA-Tyr^{3}-octreotate in a small cell lung cancer animal model. *Eur J Nucl Med Mol Imaging.* 2006;33:S114-S115.
19. Müller C, Forrer F, Bernard BF, et al. Diagnostic versus therapeutic doses of [^{177}Lu-DOTA-Tyr^{3}]-octreotate: uptake and dosimetry in somatostatin receptor-positive tumors and normal organs. *Cancer Biother Radiopharm.* 2007;22:151-159.
20. Velikyan I, Sundin A, Eriksson B, et al. In vivo binding of [^{68}Ga]-DOTATOC to somatostatin receptors in neuroendocrine tumours—impact of peptide mass. *Nucl Med Biol.* 2010;37:265-275.
21. Müller C, Brühlmeier M, Schubiger AP, Schibli R. Effects of antifolate drugs on the cellular uptake of radiofolates in vitro and in vivo. *J Nucl Med.* 2006;47:2057-2064.
22. Müller C, Schibli R, Krenning EP, de Jong M. Pemetrexed improves tumor selectivity of ^{111}In-DTPA-folate in mice with folate receptor-positive ovarian cancer. *J Nucl Med.* 2008;49:623-629.
23. Müller C, Reddy JA, Leamon CP, Schibli R. Effects of the antifolates pemetrexed and CB3717 on the tissue distribution of ^{99m}Tc-EC20 in xenografted and syngeneic tumor-bearing mice. *Mol Pharm.* 2010;7:597-604.

24. Larsson E, Strand SE, Ljungberg M, Jonsson BA. Mouse S-factors based on Monte Carlo simulations in the anatomical realistic Moby phantom for internal dosimetry. *Cancer Biother Radiopharm.* 2007;22:438-442.
25. Emami B, Lyman J, Brown A, et al. Tolerance of normal tissue to therapeutic irradiation. *Int J Radiat Oncol Biol Phys.* 1991;21:109-122.
26. Kwekkeboom DJ, de Herder WW, Kam BL, et al. Treatment with the radiolabeled somatostatin analog [^{177}Lu-DOTA^{0},Tyr^{3}]octreotate: toxicity, efficacy, and survival. *J Clin Oncol.* 2008;26:2124-2130.
27. Bodei L, Cremonesi M, Ferrari M, et al. Long-term evaluation of renal toxicity after peptide receptor radionuclide therapy with ^{90}Y-DOTATOC and ^{177}Lu-DOTATATE: the role of associated risk factors. *Eur J Nucl Med Mol Imaging.* 2008;35:1847-1856.
28. Vegt E, de Jong M, Wetzels JF, et al. Renal toxicity of radiolabeled peptides and antibody fragments: mechanisms, impact on radionuclide therapy, and strategies for prevention. *J Nucl Med.* 2010;51:1049-1058.
29. Rolleman EJ, Krenning EP, Bernard BF, et al. Long-term toxicity of [^{177}Lu-DOTA^{0},Tyr^{3}]octreotate in rats. *Eur J Nucl Med Mol Imaging.* 2007;34:219-227.
30. Weitman SD, Lark RH, Coney LR, et al. Distribution of the folate receptor GP38 in normal and malignant cell lines and tissues. *Cancer Res.* 1992;52:3396-3401.
31. Kennedy MD, Jallad KN, Lu J, Low PS, Ben-Amotz D. Evaluation of folate conjugate uptake and transport by the choroid plexus of mice. *Pharm Res.* 2003;20:714-719.
32. Wollack JB, Makori B, Ahlawat S, et al. Characterization of folate uptake by choroid plexus epithelial cells in a rat primary culture model. *J Neurochem.* 2008;104:1494-1503.